

# TRIBOLOGY ASPECTS OF THE NIRSPEC FILTER AND GRATING WHEEL MECHANISMS

Marc M. Ellenrieder<sup>1</sup>, K. Weidlich<sup>1</sup>, T. Groß<sup>1</sup>, M. Fischer<sup>1</sup>, A. Kolb<sup>1</sup>, H.-U. Wieland<sup>1</sup> and M. Trunz<sup>2</sup>

<sup>1</sup>Carl Zeiss Optronics GmbH, Carl Zeiss Straße 22, 73447 Oberkochen, Germany; m.ellenrieder@optronics.zeiss.com

<sup>2</sup>IST Ingenieurbüro für Strukturmechanik Michael Trunz, Ulmer Straße 130, 73431 Aalen, Germany

## ABSTRACT

The optical function of the Near-Infrared Spectrograph (NIRSPEC) on board the James Webb Space Telescope can be reconfigured in space by two ratchet operated cryo mechanisms. The tribological design of the mechanism's ratchet, the motor and the friction-based optical grating and prism mounts is presented. The particular challenges of the motorization margin calculation is highlighted. The breadboards for ratchet and grating mounts are presented and the lessons learned will be summarized.

Key words: Cryomechanisms, Ratchet, Tribology, NIR-Spec, Testing, JWST.

## 1. INTRODUCTION

As successor to the successful Hubble Space Telescope, the James Webb Space Telescope (JWST) is currently being built under joint responsibility of NASA, the European Space Agency (ESA) and Canadian Space Agency (CSA). It will be launched in 2013.

### 1.1. The NIRSPEC Instrument

One of the four instruments on board JWST is the Near-Infrared Spectrograph (NIRSPEC), which covers the wavelength range between 600nm and 5000nm. The NIRSPEC is being built by EADS Astrium GmbH. The NIRSPEC is a multi-object spectrograph which enables scientists to obtain simultaneous spectra of at least 100 objects in a  $> 9 \text{ arcmin}^2$  field of view. It can be reconfigured in space for astronomical observation. The NIRSPEC employs an electromechanical microshutter array for aperture control, and has two *HgCdTe*-detector arrays. To allow for low-noise operation, the NIRSPEC is passively cooled in space to a temperature in the 30 - 39K range. An overview over the NIRSPEC instrument and its mechanical design is given in a companion paper[6] and earlier publications[5]. Fig. 1 shows a design drawing of the NIRSPEC.

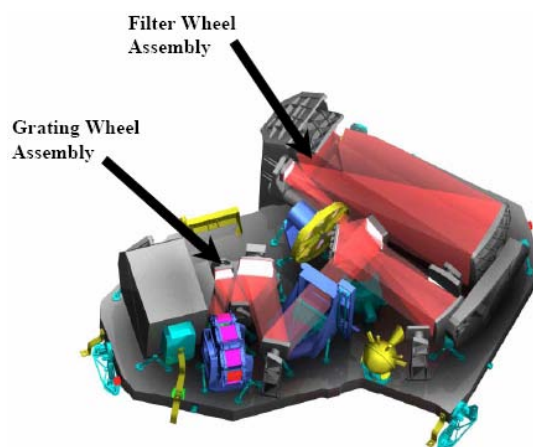


Figure 1. The NIRSPEC instrument (picture courtesy of EADS Astrium GmbH) with the Filter and Grating Wheel Assemblies.

### 1.2. The Filter and Grating Wheel Assemblies

Reconfiguration of the NIRSpec instrument will be achieved using a Filter Wheel Mechanism (FWA) and a Grating wheel assembly (GWA) which position a number of filters, gratings and a prism accurately in the optical beam path. Positioning tolerances down to less than one arcsec and one micron have direct impact on the instrument's performance. Deformation of optical surfaces must be limited to the nanometer scale. Critical load cases are full functionality under both ambient conditions and in cryo-space (30K) and high vibration loads on bearing and optical components during launch. The mechanism part of the wheel assemblies was based on space proven concepts derived from the successful ISOPHOT filter wheel mechanisms which were designed, manufactured and tested by CARL ZEISS. Implementation of the NIRSpec filter and grating wheels is under responsibility of CARL ZEISS OPTRONICS which involves manufacturing of the wheel structures complete with optical components and assembly level tests. Major subcontractors are RUAG AEROSPACE AUSTRIA and MAX-PLANCK-INSTITUT FÜR ASTRONOMIE, Heidelberg, (MPIA) which contribute the mechanism support structure (MS) with the central duplex bearing and the

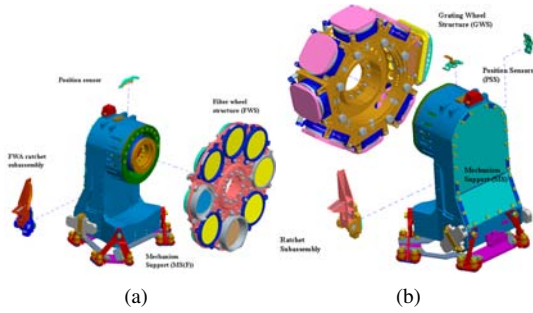


Figure 2. The Filter (a) and Grating Wheel (b).

electrical subassembly respectively. Mechanical and FE design was done in cooperation with the INGENIEUR-BÜRO FÜR STRUKTURMECHANIK MICHAEL TRUNZ, AALEN.

The mechanisms use a mechanical ratchet with flexural pivots which slides on eight index ball bearings mounted to the wheel in order to provide 2.5 arcsec repeatability of the 8 optical positions. The ratchet is also used to maintain the wheels position during launch and in un-powered condition.

The paper will only present a brief overview on the design, as this has been described in other publications[1, 7, 9, 8]. Instead, the main focus of the presented paper lies in the tribology aspects and the lessons learned from breadboard and flight testing. This comprises design and test aspects of the ratchet mechanism with respect to motorization, lifetime, general tribology including motorization, and coating. The design and performance of the optical mounts which hold the optics by friction only, is also presented. An earlier paper [3] and a companion publication within this proceedings volume [4] describes the novel central duplex ball bearing contained within the mechanisms. Fig. 2 shows an overview of both mechanisms.

## 2. MOTORIZATION CONCEPT

Both FWA and GWA share the same motorization philosophy. The mechanisms have two actuators:

- a fully-redundant, space-proven and cryo-capable electrical motor, type C116 manufactured by TTL, and
- a double-coiled spring-operated ratchet with a redundant pair of flexural pivots.

Both actuators complement each other. The mechanism is not able to function without either one. In §2.2, the motorization concept will be described in more detail. Fig. 3b shows all actuators and torque contributing effects.

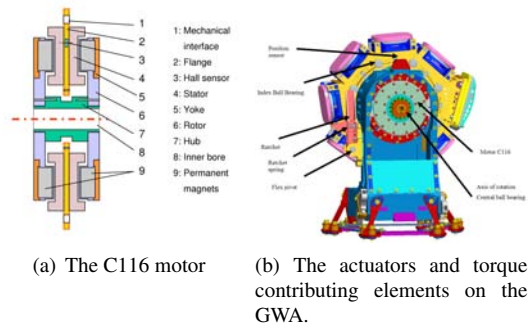


Figure 3.

The fact that the mechanism shall be safely powered by both the ratchet and the motor is particularly challenging for the calculation of the motorization margin: if the ratchet operates the mechanism, it needs to be dimensioned such that it can overcome all torque contributions. As the motor is completely brush-less and does not contain metallic parts within the stator, there is no breaking torque of the unpowered motor and the ratchet does not need to work against it. However, in case of motor operation, the ratchets torque will need to be overcome by the motor, making power consumption a very big challenge.

### 2.1. Motor C116

The C116 is a larger version of the C84 motor from TIEFTEMPERATUR LABORATORIES (TTL) at the FU Berlin that is utilized as actuator in all MIRI mechanisms. The general torque motor family Cxxx from TTL was developed in the early 1980s for cryogenic applications and has been utilized in a number of cryogenic applications and space missions including HERSCHEL. The design is simple by configuration and does not contain any bearings. This provides for safe operation under cryogenic conditions. The torquer is a two-phase motor which is operated by calibrated wave-forms (fractions of sine and cosine). The motor will move the wheel between adjacent angular positions where the motor drive scheme takes reference from the positioning ratchet for accurate synchronization without needing a position measurement. Between adjacent wheel positions which are  $2\pi/8$  radian apart, the motor drive scheme needs to be optimized to safely realize the trajectory between adjacent start and target angular positions taking into account the wheel's dynamic parameters such as moment of inertia, friction (bearing torque) and the fluctuations and tolerances as well. These will be dealt with by applying the appropriate ECSS factors for motor operation.

### 2.2. Operational Modes of the Mechanisms

The mechanisms can be operated in two modes and especially the ratchet must be designed such that both can be used efficiently. The first operational mode is called

*microstepping mode* where a constant current amplitude is applied to the motor such that it drives the wheel with constant angular velocity and constant torque. This mode is the default, as it is the most robust with respect to torque variations and limits the angular momentum to very low values, making instrument or even telescope disturbance negligible. However, it discards the driving power of the ratchet and consumes a lot of electrical power which leads to high dissipation, which is undesirable in a cryogenic instrument. The second mode is called *torque mode*. In this mode, the motor is operated with a time dependant current amplitude which applies a high torque at the beginning of the movement and until the ratchet has overcome its dead position. The controller software then reduces the motor current and relies on the ratchet as the main actuator. The motor is even used to apply a breaking torque to reduce the oscillation of the wheel around its end position and to allow for a much shortened settling time. The drawback of this mode is the relatively high angular momentum at the beginning of a movement and the slightly lower robustness towards torque variations over time in a non-closed loop controlled mechanism. However, the power dissipation is very low and the wheel can move much quicker. Both modes are fully ECSS compatible.

### 3. RATCHET

Both FWA and GWA are equipped with a spring-operated ratchet. The ratchet provides the following functionality:

1. Ultimate angular repeatability of operational positions of respective optical components
2. Provides the actuation power for drawing the wheel into its final accurate position after the torque motor has switched off close to target position.
3. Well-defined torque over angular wheel position during repositioning which is utilized for optimization of the repositioning transient
4. Holding the un-powered mechanism in nominal position during launch and during observation
5. Driving the wheel to a defined end position, if the motor fails.

The accuracy which is required for angular positioning (repeatability, stability) of optical components translates into micron (and even sub-micron) dimensions, if the size of the GWA is taken into account. The required repeatability of 2.5 arcsec angular deviation correspond to  $1.2\mu\text{m}$  tangential shift on a 100 mm radius. The angular accuracy about the mechanism's axis of rotation relies on a custom designed flexural pivot. This concept has been successfully employed at ZEISS in two earlier space missions, namely ISOPHOT and HERSCHEL's PACS chopper. It is also employed for the current JWST MIRI filter and dichroic wheel mechanisms [2].

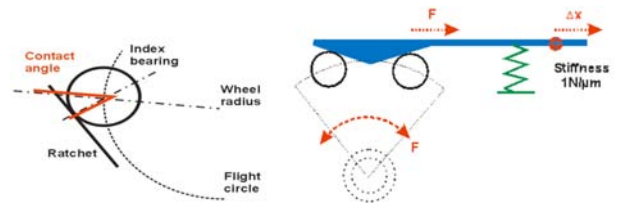


Figure 4. Forces on the flexural pivot.

#### 3.1. Accuracy at ambient and cryo vs. torque

Stationary accuracy of the mechanism, i.e. when the ratchet is engaged, is governed by four factors:

1. The central ball bearing torque and the stiffness of the ratchet's flexural pivot
2. The alignment accuracy of the ratchet's nominal position (for absolute positioning)
3. The radial run out of the index ball bearings (for repeatability)
4. The overall tolerances on mechanism support and wheel level, including the misalignment of the central ball bearing's axis of rotation

The holding torque which is applied by the ratchet, however, does not come into play, as long as the force pressing on the index ball bearings it is larger than the force needed to squeeze out their gapping. Points 2 to 4 can be considered as fixed during the mission and need no further explanation. Point 1 can be explained by Fig. 4: when the ratchet engages in one position, it is no longer possible to distinguish between a movement of the ratchet arm in tangential direction due to the finite stiffness of the flexural pivots and an unfinished movement of the overall wheel. The force deforming the flexural pivot is directly proportional to the central ball bearings running torque. This means, the effect is much worse at ambient than at cryo and it is a major factor for attaining ambient accuracy. Increasing the holding / driving torque of the ratchet itself does in no way ameliorate this situation and will therefore not give a better ambient accuracy. Hence, no additional holding torque for accuracy at ambient and cryo was factored into the motorization calculation.

#### 3.2. Tribological Ratchet Design

The ratchet profile must be properly designed to provide a predefined torque to the wheel disks for each angular wheel position. The angular torque function is presented below. The ratchet torque can be changed by changing a spring force included to the ratchet subassembly, providing a means to adjust the wheel's dynamic parameters and, in particular, the relation between bearing friction torque and ratchet torque. In addition, the ratchet profile

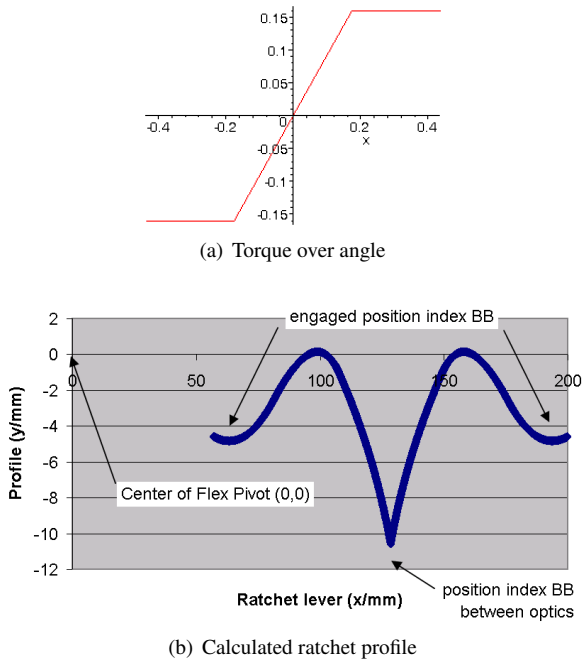


Figure 5.

Table 1. Torque contributions for motorization margins

| Parameter                                       | Value | Unit |
|---|-------|------|
| Avg. bearing torque @ ambient                   | 60    | Nmm  |
| Avg. bearing torque @ cryo                      | 15    | Nmm  |
| Ratio between peak and avg. torque after run-in | 2     |      |
| Max breaking torque on wheel due to index BBs   | 4     | Nmm  |
| Dynamic resistive torque                        | 30    | Nmm  |
| Ratchet torque measurement tolerances           | +/-10 | %    |
| Min. ratchet spring stiffening cryo vs. ambient | 8     | %    |
| Max ratchet spring stiffening cryo vs. ambient  | 20    | %    |

/ driving torque must be such that no overshooting occurs which will lead to a high angular momentum. The ratchet's actuated torque needs to be adapted to the overall torques of the wheel: in order to guarantee safe motor operations within the motor and ICE-box limits, the ratchet's profile needs to be adapted. Ideally, the ratchet torque is constant over the whole angular range between two nominal positions, i.e. positions where an optical element is properly positioned, with a linear transient about the dead center position of the ratchet. The maximum required torque needs to be calculated by using the applicable ECSS formulas. The values from Tab. 1 were used as input for the calculation. In order to avoid stacking of margins in the motorization margins for ratchet and motor operation, the ECSS factors were reduced with ESA concurrence from their nominal ones. This results in a symmetrical torque profile for both directions of rotation, cf. Fig. 5a, with a maximum torque of 160Nmm at ambient temperatures. The torque of the ratchet will increase due to the stiffening effect of the spring constant to 176Nmm, cf. Fig. 6. By modeling the geometrical relations of the ratchet during turning of the wheel and integrating the re-

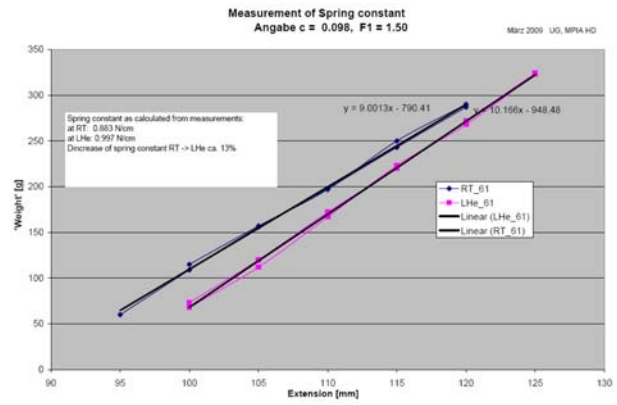


Figure 6. Spring constant over temperature

sulting equation the profile of the ratchet could be calculated, cf. Fig. 5b. For manufacturing reasons, the profile was smoothed at the position of the index-ball bearing for the fully deflected ratchet. For comparison, the ECSS calculations result in a motor torque of about 600Nmm that is needed to safely overcome the wheel friction and the ratchet. Due to the ECSS factor logic which applies a factor of 1.2 to the already over-dimensioned ratchet and then sums up the other torque contributions (with possibly reduced factors due to a friction measurement) friction of the central duplex ball bearing is nearly negligible for the motor calculation and only the ratchet's actual torque is relevant.

### 3.3. Mechanical Ratchet Design

To better understand the employed breadboard program, a short description of the mechanical ratchet design is given. The ratchet assembly includes the ratchet lever arm with end stops to limit the maximum deflection under vibration, a redundant double coiled spring a pair of flexural pivots and an alignment mechanism. Fig. 7 shows the ratchet assembly and the flexural pivot. The latter is a monolithic design which is manufactured from a single rod of material. The critical features of the flexural pivot are the crosses blades whose thickness and length are critical structure parameters. Both titanium alloy Ti-Al6-V4 and copper beryllium CuBe2 are suitable materials for the flexural pivots according to a study performed in the PACS program. Both materials were also tested for NIR-Spec within the breadboard programme. Because the flex pivots are potential single point failure items, they have to be submitted to particular inspections in order to assess their integrity after machining. In general, resistance of Ti-Al6-V4 and CuBe2 to fatigue and crack propagation is excellent. Like most titanium alloys, Ti-Al6-V4 has outstanding resistance to corrosion. Because the flexural pivot's stiffness differs strongly in both directions perpendicular to its symmetry axis the flexural pivot must be properly oriented in the ratchet mount.

Two pairs of crossed blades are the major functional el-

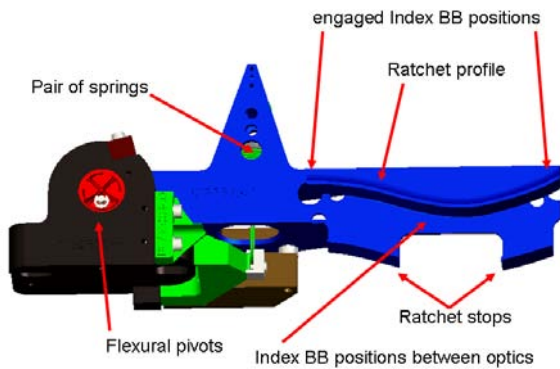


Figure 7. The NIRSpec ratchet with the detent (blue).

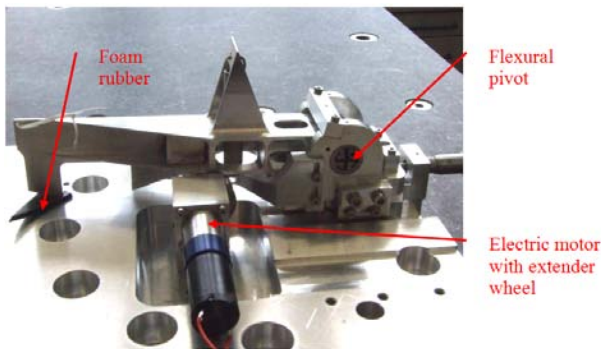


Figure 8. The NIRSpec ratchet during BB lifetime testing

ements of the flexural pivot. The blades allow for bending. The perpendicular configuration of blades constrain the bending of blades to a well-defined axis. The flexural pivot provides two fixation rings which are only connected by the crossed blades and a connecting bar between the pairs of crossed blades. Departure from central axis is limited to less than 100 nm for pivot angular range of  $\pm 9^\circ$ . The flexural pivot is made from a single piece of alloy material. No welds or clamping connections are used in the functional part. The design is therefore suitable for application at cryogenic temperature and over the large temperature range needed for the NIRSpec instrument. Two flexural pivots establish the hinge for the ratchet detent. Axis of both pivots have to be accurately aligned to avoid shearing stress during operation. This is realized by a tight fit and a connecting pin. The distance between flexural pivots and a lateral end stop is used to adjust torsional stability under vibration load.

#### 4. BREADBOARD TESTING OF THE RATCHET

The ratchet and the index ball bearings were subject to an extensive breadboard programme. The breadboard consisted of several tests regarding repeatability accuracy, actuating force, lifetime and vibration. For this a breadboard ratchet was built and tested in several configurations, cf. Figs. 8, 9, and 10. All tests were done with

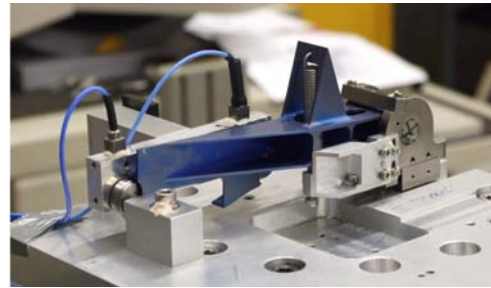


Figure 9. The BB ratchet during vibration testing

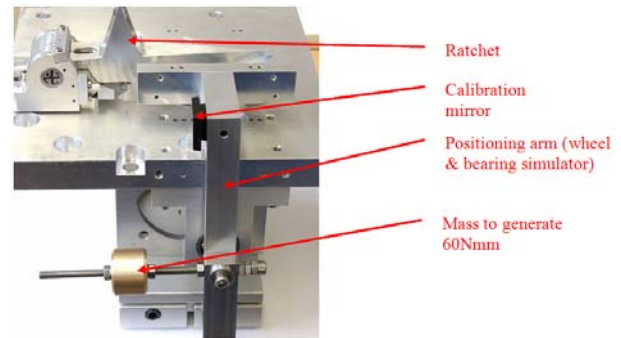


Figure 10. The ratchet BB repeatability setup

a Ti-Al6-V4 and a CuBe2 flexural pivot. Because of a potential CTE mismatch between the Ti-Al6-V4 ratchet lever and the pivot, the Ti-Al6-V4 pivot is the baseline option.

##### 4.1. Flexural Pivot

In general, it can be stated that the structural design of the flexural pivot itself was very critical. Even more, since the manufacturing methods that are available to machine the pivots do not tolerate any variation. Several attempts had to be made to achieve the necessary surface smoothness of the Ti-pivot's  $150\mu\text{m}$ -thick blades during wire erosion: it was found during vibration and lifetime testing, that the roughness of the pivot's blades is crucial for their stability under load, something which cannot be modelled properly in a FE design. In a first step, the corner radii were enlarged and the pivots were surface treated to remove any remaining roughness and thus stress. However, this proved to be difficult due to the complicated geometry and the rather thin blades. The fracture resistance of the Ti-alloy was also critically lowered and the pivot did not survive vibration any more. In a parallel attempt, the manufacturer tried to use different erosion techniques to obtain minimal surface roughness of the cut areas. Only after several process optimizations, the correct procedure could be found. With CuBe2 that was manufactured in parallel there was no such problem. Both Ti and CuBe2 flexural pivots were installed in a ratchet for vibration, repeatability and lifetime testing. Both flexural pivots showed sufficient performance, with the Ti pivots slightly better in repeatability (probably due

to the higher stiffness in ratchet lever direction, cf. Fig. 4) and the CuBe2 pivots with less problems during vibration and lifetime. As the CTE problem between CuBe2 pivot and Ti-alloy detent was difficult to solve within the existing hardware, the decision was maintained to use the Ti-alloy as baseline solution.

#### 4.2. Ratchet profile

During vibration and lifetime testing, the ratchet profile and the index ball bearings were subjected to rattling shocks and sliding. However, for the sake of a conductive path between ratchet and wheel, no lubrication was chosen: neither on ratchet profile nor within the index ball bearing. Another reason for that is the fear of particles close to the optical elements that are generated by the lubrication either under vibration or under normal use. Therefore, during breadboarding particular focus was given to these components and their wear and tear. During breadboard testing at 120% vibration levels, the ratchet's profile showed only very light marks but without impact on repeatability. Per design, the maximum force from the ratchet onto the index ball bearing is 2.5N. This rather low force and the accompanying contact areas make sure, that cold welding is not an issue, when the mechanism is not operated for a long time. This was also proven by a pin-disk test. To further reduce the risk of cold welding, the Ti-lever arm was anodised. By design, it was also made sure, that even in the case of blocking index ball bearing, the resulting breaking torque would not surpass the values given in Tab. 1.

### 5. FRICTION BASED MOUNTING OF THE OPTICAL ELEMENTS

The optical elements of the filter and grating wheel and their mounts are described in detail in [1]. Of particular interest from a tribology point of view are the grating and prism mounts. The grating mounts are made from Titanium alloy Ti6Al4V which provides an intermediate CTE between the Aluminium alloy material of the grating wheel structure and the nearly zero expansion of the ZERODUR material of the grating substrate. Adjusting screws were implemented on the grating mount in order to correct the alignment error between the optical components of the after assembly down to less than 30 arcsec at operational temperature. By structural design, the mechanical stress in the optical mount resulting from different alignment states of the screws shall not significantly influence the WFE of the optics. The substrate is held by friction only between two membranes and centered by three sapphire alignment balls, cf. Fig. 11. The cross-section runs through the mounted grating along the central axis. The viewgraph shows details of the assembly along the clamping ring. The detailed design of the clamping interface depends critically on the friction coefficient of the grating to mount interface. In order to keep the grating in place under vibration load,

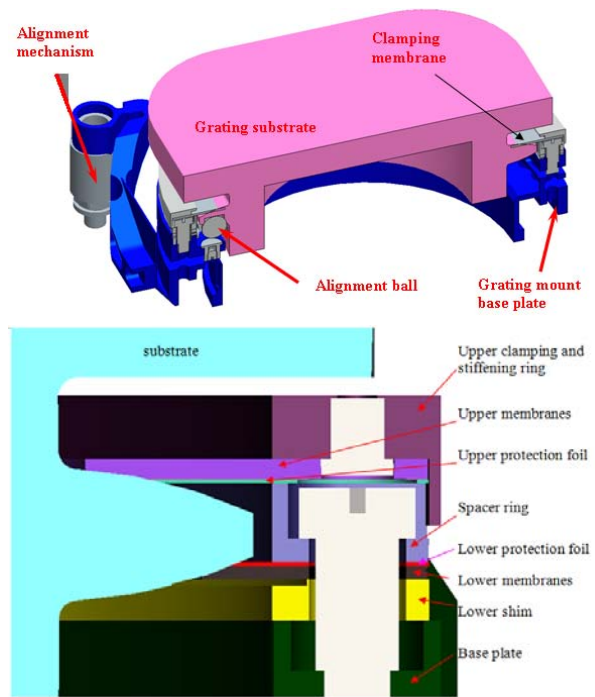


Figure 11. Cross section through mount with substrate (top) and closeup of the clamping interface.

the contact areas between clamping ring and grating substrate are properly finished in order to provide for sufficient friction for the selected clamping force. The upper and lower clamping membranes are thin blades made of Ti6Al4V and are relatively stiff. There are up to three upper and lower membranes which need to be combined in accordance with the required preload, the friction coefficient, the available blade thicknesses and the overall WFE of the mount. The final configuration was found by extensive FEM calculation and complementing breadboard activities. The spacer ring is used to further adjust the preload on the substrate. The lower shim is used to adjust the z-position of the grating in accordance with the thickness of the lower membrane stack: The contact angle between the membranes and the substrate are critical with regard to the induced WFE and local stress on the substrate. To pad the contact area, to avoid abrasion in the contact areas during vibration or cryo cooling, and to reach a near perfect line of contact around the substrate, a very thin pure titanium protection foil is inserted between each clamping membrane and substrate. This is especially critical for the lower membrane stack, where the contact angle between membranes and substrate is higher than on the upper side.

For brevity reasons, the prism mount is not presented in detail here, but in [1]. However, for holding the CaF2 prism knowledge of the friction coefficient between the glass material and the holding spring membranes is considered equally critical.

Table 2. Summary of measured friction coefficients

| No | Glass substrate | Membrane                              | Pulling speed | Test Weight     | $\mu H$   | $\mu G$   |
|----|-----------------|---------------------------------------|---------------|-----------------|-----------|-----------|
| 1  | Zerodur, lapped | CA foil                               | 5mm/min       | 13,73N          | 0,18      | 0,11      |
| 2  | Zerodur, lapped | Kapton foil                           | 5mm/min       | 13,73N          | 0,25      | 0,14      |
| 3  | Zerodur, lapped | Ti-6Al-4V, fine ground                | 1 - 10 mm/min | 48,67N          | 0,13      | 0,13      |
| 4  | Zerodur, lapped | Ti-6Al-4V, fine ground w/ NiP plating | 5mm/min       | 13,73N & 23,36N | 0,15-0,18 | 0,12-0,14 |
| 5  | CaF2 polished   | Ti-6Al-4V, fine ground                | 5mm/min       | 11,69N          | 0,27      | 0,20      |
| 6  | CaF2 polished   | Ti-6Al-4V, fine ground                | 5mm/min       | 21,33N          | 0,23      | 0,20      |
| 7  | CaF2 polished   | Ti-6Al-4V, fine ground w/ NiP plating | 5mm/min       | 11,69N          | 0,18      | 0,14      |

Table 3. Summary of vibration tested membrane combinations for grating mount

| No | Upper m.               | Lower m.                       | Protection Foil                  | Result  |
|----|------------------------|--------------------------------|----------------------------------|---|
| 1  | Single, thick Steel m. | Single, thick Steel m.         | None                             | Severe abrasion   |
| 2  | Single, thick Steel m. | Single, thick Steel m.         | Kapton foil or cellulose acetate | No abrasion, but high stick-slip behaviour. High influence of I/F tolerances      |
| 3  | Multiple thin Steel    | Multiple thin Steel            | Kapton in different thicknesses  | No abrasion, but high stick-slip behaviour. Much less influence of I/F tolerances |
| 4  | Mult. thin Ti6Al4V     | Mult. thin Ti6Al4V             | 10 $\mu$ m-Ti foil               | No abrasion, good friction control. Very little influence of I/F tolerances       |
| 5  | Mult. thin Ti6Al4V     | Mult. thin Ti6Al4V, NiP plated | none                             | Hard to get correct foil thickness<br>High abrasion                               |

## 6. BREADBOARD TESTING OF THE OPTICAL MOUNTS

The structural analysis of the mechanism called for a necessary force of 120N in lateral direction to safely hold the grating substrate in place. For the prism a similar assessment was made. Hence, the goal of the test activities was to achieve the necessary axial preload with a suitable combination between axial preload and the friction coefficient. Several configurations of material combination were tested to ascertain the correct friction coefficient and to make sure, that the glass substrate will not be damaged by the membranes during vibration. In principle, the membrane material, their number and thicknesses as well as the surface finish of the membranes were compared. In addition, the effect of a protection foil was investigated. This protection foil would be placed between the membranes and the substrate so that the contact pressure is evened out and sharp edges from cutting the membranes would not scrape the glass. The protection foil material would significantly influence the friction coefficient and thus the necessary axial preload. Some of the tested combinations are listed in Tab. 3. For each combination, the thickness of the membranes was chosen such that the calculated preload would be sufficient to hold the substrate under vibration with an assumed friction coefficient. The friction coefficient was tested with a small tribological setup shown in Fig. 12. The obtained friction coefficients are given in Tab. 2. The test force for each measurement was chosen to represent the expected force in the

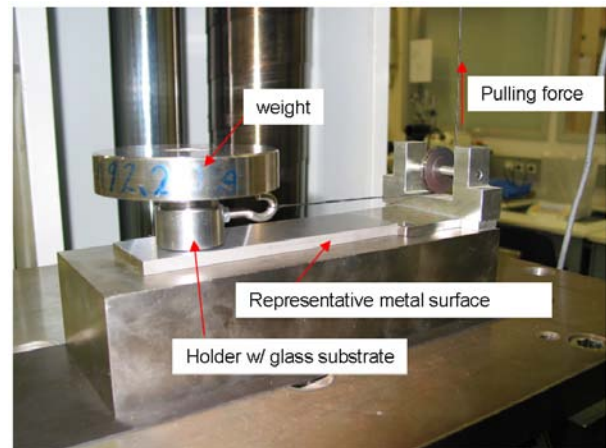


Figure 12. Cross section through mount with substrate (top) and closeup of the clamping interface.

mount prior the measurement. During vibration, the friction coefficient was then reconfirmed by increasing the static vibration load until the friction would be overcome. If this was not feasible, the substrate would be laterally pushed by a dedicated GSE which cuts the pushing force as soon as the substrate moves. After vibration testing the decision was taken to use configuration no. 4 from Tab. 3, because the tribological behaviour was found to be the best of all tested configurations. The big challenge that remained was to obtain Ti-membranes with the necessary thicknesses, as the available standard thicknesses were not well suited. This problem could not be solved to full satisfaction. Trials to produce tailored thicknesses by chemical etching were done, but the process was difficult to control. In the end, the decision was taken to choose the closest standard thickness and sacrifice some WFE due to the slightly higher preload.

## 7. LESSONS LEARNED & CONCLUSION

As a short summary, the following lessons learned can be stated:

- Motorization for a ratchet operated mechanism is critical. The ECSS logic is not particularly apt to deal with such mechanisms and must be tailored with ESA concurrence for the actual case. Without a pre-load off-loading, the motorization would not be feasible.
- Wire erosion of Ti-6Al-4V alloy in thin structures is a very critical process and needs to be accompanied by extensive breadboard testing
- Friction testing is mandatory if the design is critical.
- Friction coefficient measurements must be confirmed by independent measurements
- An intermediate protection foil or cushion is beneficial for low abrasion if a delicate (glass) substrate is held by an elastic membrane.
- An optical mount which relies only on friction is difficult to tune. Hard mounting is preferable.

The upcoming flight hardware testing campaign will demonstrate, whether the design assumptions and the lessons learned during breadboarding hold true. It is expected, that some of the results can already be presented in the accompanying talk during the symposium. The main author may be contacted via e-mail to obtain a copy of the presentation.

## 8. ACKNOWLEDGEMENTS

The presented work is the result of the recent work performed at CARL ZEISS OPTRONICS GmbH, the INGENIEURBÜRO FÜR STRUKTURMECHANIK TRUNZ (IST),

Aalen, and the MAX PLANCK INSTITUTE FOR ASTRONOMY, Heidelberg. The authors would like to thank all people who have participated in the NIRSPEC mechanism project, especially the AIV team at CARL ZEISS OPTRONICS.

## REFERENCES

1. M. M. Ellenrieder, K. Weidlich, B. Nelles, B. Ploss, S. Bruynooghe, J. Koehler, and M. Te Plate. The optical components of the NIRSpec wheel mechanisms. In *Proc. SPIE Astr. Inst.: Adv. Opt. & Mech. Techn. in Telescopes & Instr.*, volume 7018, Marseilles, June 2008.
2. O. Krause, F. Müller, and S. Scheithauer. Wheel mechanisms of the mid-infrared instrument aboard the James Webb Space Telescope - performance of the flight models. In *Proc. 13th ESMATS*, Vienna, Austria, September 2009.
3. C. Neugebauer et al. High precision duplex bearing with thermal offload device for the NIRSpec wheel support mechanisms. In *Proc. 12th ESMATS*, Liverpool, UK, September 2007.
4. C. Neugebauer and L. Supper. NIRSpec wheel support mechanisms central duplex bearing cryogenic test results. In *Proc. 13th ESMATS*, Vienna, Austria, September 2009.
5. W. Posselt, W. Holota, G. Kulinyak, et al. NIRSpec: Near infrared spectrograph for the JWST. In J. C. Mather, editor, *Proc. SPIE: Astronomical Telescopes and Instrumentation*, volume 5487, 2004.
6. J.-C. Salvignol, K. Honnen, and R. Barho. JWST NIRSpec Mechanical Design. In *Proc. SPIE Astr. Inst.: Adv. Opt. & Mech. Techn. in Telescopes & Instr.*, volume 7018, Marseilles, June 2008.
7. K. Weidlich, M. Ellenrieder, et al. Breadboard testing for the JWST NIRSpec grating and filter wheels. In *Proc. 12th ESMATS*, Liverpool, UK, September 2007.
8. K. Weidlich, M. Ellenrieder, et al. High-precision cryogenic wheel mechanisms for the JWST NIRSpec instrument. In *Proc. SPIE Astr. Inst.: Adv. Opt. & Mech. Techn. in Telescopes & Instr.*, volume 7018, Marseilles, June 2008.
9. K. Weidlich, M. Sedlacek, M. Fischer, M. Trunz, M. Ellenrieder, et al. The grating and filter wheels for the JWST NIRSpec instrument. In *Proc. SPIE: Optomechanical Technologies for Astronomy*, volume 6273, Orlando, July 2006.